Integrated hydrogeochemical and geophysical surveys for a study of sea-water intrusion

P. Capizzi, D. Cellura, P. Cosentino, G.Fiandaca, R. Martorana, P. Messina, S. Schiavone and M. Valenza

Department of Chemistry and Physics of the Earth (CFTA), Palermo, Italy

(Received: December 30, 2009; accepted: June 22, 2010)

Abstract The CFTA Department of the University of Palermo in collaboration with ARPA SICILIA has carried out a study of the sea intrusion phenomenon in the aquifer between the cities of Marsala and Mazara del Vallo (south-western Sicily) using geophysical techniques (TDEM, ERT and MASW) and geochemical analysis of well water. The aim of the research was to optimize the acquisition techniques, data processing and data interpretation for the geometry reconstruction of aquifers, their characterization, and the determination of concentration of pollutants. The analysis of the geophysical results reveals the existence of very low resistivity values in correspondence of the area from the coastline to a kilometer inland. Obviously, in this area, the sea intrusion is more pronounced. Furthermore, major element contents and physical-chemical parameters of sampled water testify that the main process that defines the groundwater geochemistry in this area is a mixing between the carbonatic aquifers and the marine component. A significant contamination of nitrate and sulphate is also present. About 90% of the sampled wells were contaminated over the Italian legislation limits.

1. Introduction

The increase of the phenomenon of sea water intrusion, due to the excess of water withdrawals, and agricultural, industrial and/or chemical contamination represent the major risks for coastal aquifers. The environmental damage caused by overuse of coastal aquifers is also related to changes in ecosystems due to the reduction of water discharge in streams, wetlands and coastal estuaries; contamination of groundwaters, when not directly toxic for the coastal ecosystems, often causes the introduction of excess nutrients (nitrogen and phosphorus), responsible for the alteration of the natural equilibrium (National Research Council, 2000). For these reasons public administrations have to take into account the degradation of water quality and the decrease in the amount of groundwater in storage to develop a sustainable management of groundwater resources, especially in coastal areas where sea water intrusion enhances these problems. Recent Italian modifications to legislation (legislative decree n. 152 of 2006) introduced the obligation, for regional administrations, to study the quality and the state of exploitation of the hydrogeological basins, in order to plan sustainable use of groundwater resources, even against desertification. In this contest, the C.F.T.A. Department of University of Palermo, in collaboration with the ARPA SICILIA (the Sicilian agency for environmental protection), has carried out a study (Cosentino *et al.*, 2007)of the sea intrusion phenomenon in

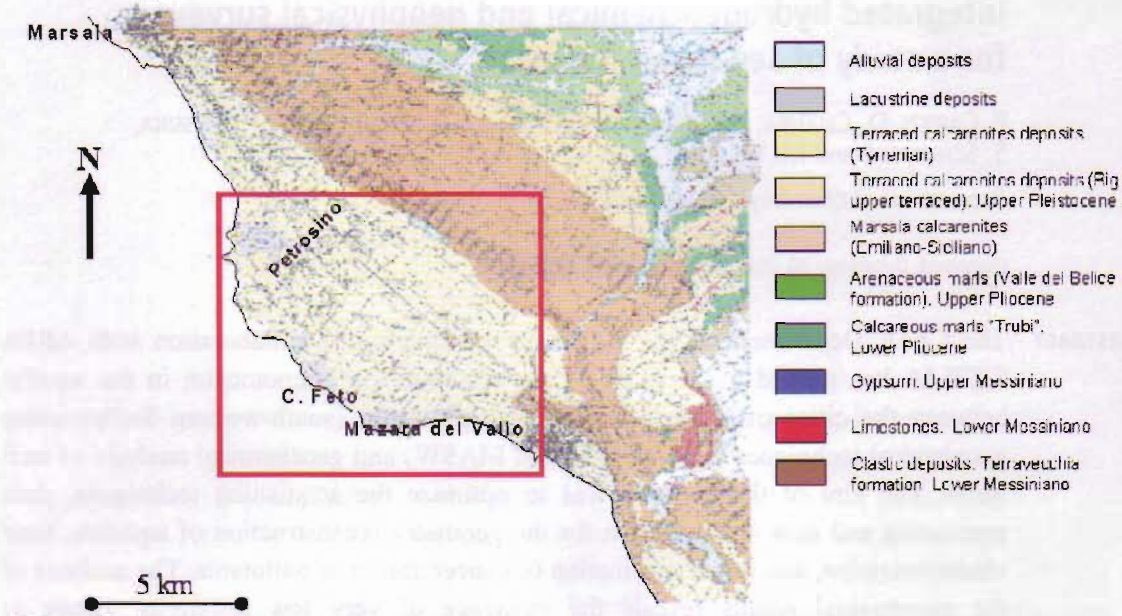

Fig. 1 - Geological map (D'Angelo and Vernuccio, 1992). The red square indicates the studied area.

the coastal area between the cities of Marsala and Mazara del Vallo (south-western Sicily). This area was chosen as a test site to optimize acquisition techniques, data processing and data interpretation for the geometry reconstruction of aquifers and their characterization using geophysical and geochemical techniques. The groundwater resources are used mainly for agriculture (wine and vegetables) and as drinking-water supplies for the surrounding cities and towns. The growing water exploitation over the last decades caused the disappearance of a typical humid coastal habitat, the so-called "margi", in which the near surface groundwater emerges close to the sea, forming a brackish habitat. Furthermore, the equilibrium between salt and fresh groundwater shifted from the coast line, in the margi area, inland towards the cultivated zone, which meant that the wells nearest to the sea were abandoned. The aquifer extends for approximately 150 km^2 (Fig. 1) and is composed of Pleistocenic sand and calcarenite deposits on a clay-sand substratum (D'Angelo and Vernuccio, 1992).

2. Geophysical survey

The utilization of the time domain electromagnetic method (TDEM) for hydrogeological applications has dramatically increased during the last years. In particular, the effectiveness of this method on the study of seawater intrusion in coastal aquifers is testified by various case histories (Fitterman and Stewart, 1986; Hoekstra and Blohm, 1990; Goldman *et al.*, 1991; Kafri *et al.*, 1997).

This methodology is based on a step-wise current flowing in a transmitting loop that produces a transient secondary electromagnetic field in the underground. This, in turn, induces a change in voltage on a receiver coil. The interpretation of the shape of the decay curve, related to the

Boll. Geof. Teor. Appl., **51**, 285-300

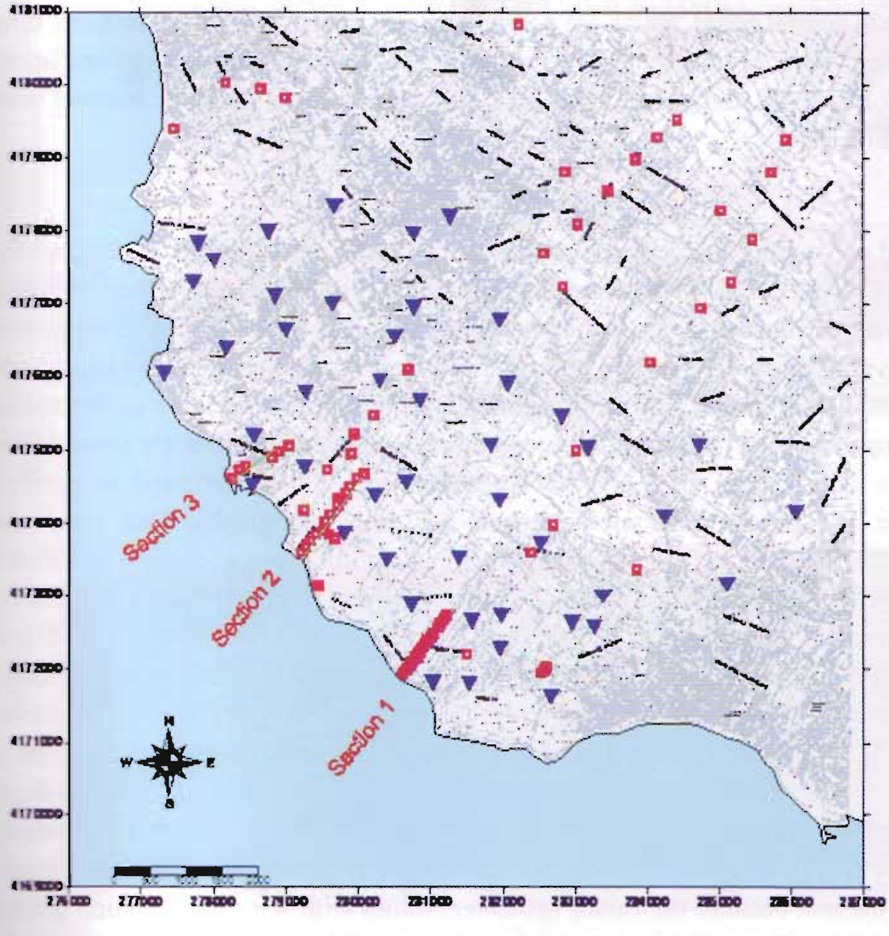

Fig. 2 - Geophysical and hydrogeochemical monitoring network.

underground resistivity distribution, allows us to obtain 1D resistivity models. The uncertainty of the estimation of the shallower layer parameters can be reduced by an a priori constraint derived from geological and hydro-geological information and other geophysical data. In this regard, combined application of d.c. and electromagnetic methods (Yang *et al.*, 1999) has been successfully used to study coastal aquifers.

The multichannel analysis of the surface waves (MASW) method (Park *et al.*, 1999; Xia *et al.*, 1999) is a non-invasive geophysical technique that uses the dispersive characteristic of Rayleigh waves to determine vertical shear-wave velocity of near-surface soil. Acquisition of experimental data is carried out using a standard seismic source (sledgehammer) and a series of low frequency geophones. The spectral analysis of the phase velocity of Rayleigh waves is studied to determine their dispersion curve with the frequency. Finally, this curve is inverted thus using it to obtain the vertical profile of the shear-wave velocity.

In order to obtain a three-dimensional model of the aquifer and to reconstruct the shape of the wedge of the sea water intrusion in the coastal zone, integrated geophysical surveys have been carried out. In particular, 53 TDEM surveys have been performed, distributed in the entire area of the aquifer, while in coastal zones, which are particularly sensitive to sea water intrusion, three detailed survey lines were reconstructed, using integrated electromagnetic investigations (TDEM), electrical resistivity tomographies (ERT) and multichannel analysis surface wave profiles (MASW) (Fig. 2).

2.1. Section n° 1

The first detailed survey line was acquired perpendicular to the coast line, up to 1250 m from the coast line: 8 ERT and 23 TDEM were carried out (Fig. 2); furthermore, 2 Vertical Electrical Soundings (VES) were carried out to verify the interpretation model of the TDEM investigation. The geoelectrical investigations were carried out with the Syscal Pro equipment (Iris Instruments, France), with 48 channels 2 spaced, in multichannel acquisition. The first three tomographies (from the sea) are superimposed for half of their length, while the other profiles are about 150 m one from the other. The Linear Grid array (Fiandaca *et al.*, 2005) was used to perform measurements, with 565 programmed measurements for each tomography. This array was developed in order to minimize the number of different current injections necessary to obtain a good resolution power. Only 13 current dipoles (and only 9 current electrodes) are sufficient for a 48-channel tomography. The capability of this array to retrieve correct interpretation models in comparison with classical array-like Wenner-Schlumberger and dipole-dipole was previously studied both with simulations and a direct comparison of results in the first 200 m of the survey line (Martorana *et al.*, 2009). The measured values of apparent resistivity range from fractions to hundreds of Ω·m, with higher values at shallower pseudo-depth, while at a deeper pseudo-depth the apparent resistivity increases from the sea line towards the cultivated land [with pseudo-depth defined as Edwards (1977)]. Measurements of apparent resistivity present a higher noise content in the profiles near the sea, because the values are lower: values with standard deviation greater than 10% (calculated by the instrument repeating the measurements) were discarded for subsequent analysis (about 30% of the measurements were discarded in the first three profiles, about 20% in the following three profiles, less than 5% in the remaining two profiles). The data were inverted by RES2DINV software (GEOTOMO Software). Inverted models are shown in Fig. 3a: the models present a stratification, with a resistive overburden on a more conductive layer. The conductivity of the deeper layer ranges from about 1 Ω·m near the coast line to tens of Ω·m: this layer has been interpreted as the saturated zone of the aquifer, with the lateral variation of resistivity justified by different contents in salt concentration. Following this interpretation, resistivity values of about 1 Ω·m correspond to a portion of the aquifer totally intruded by the sea water. In fact, the resistivity of sea water in this area of the Mediterranean Sea is about 0.2 Ω·m (Janz and Singer, 1975), and the calcarenite of the basin are much more porous (the porosity is above 20%): applying Archie's law (Archie, 1942), values around 1 Ω·m practically represent salt water.

To corroborate the interpretation coming from geoelectrical measurements, 23 TDEM soundings were performed, in order to reach a greater investigation depth. The Tem-Fast 48HPC (AEMR) instrument was used to carry out measurements, with a squared loop 25 m · 25 m. The data acquisition was made with a transmitting current of 3A and a time range of 2048 μs. All the 23 TDEM soundings were interpreted with TEM-RESEARCHER software (AEMR), imposing a

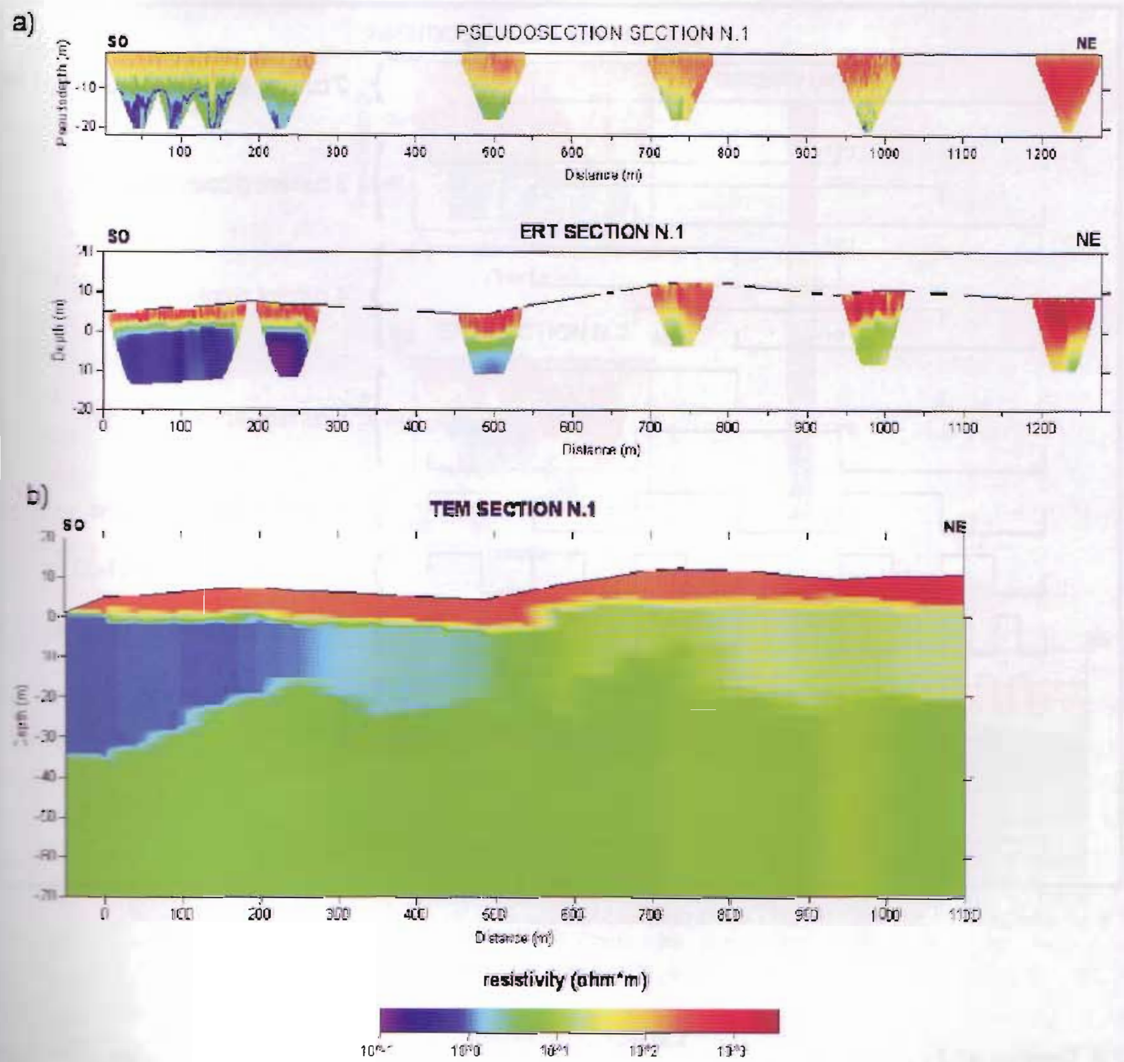

Fig. 3 – 2D interpretation of ERT survey (a) and TEM soundings (b) relative to Section n°1.

3-layer interpretation model and fixing the resistivity of the first layer equal to the main value obtained from the ERT profiles. The 1D interpretation models, jointed in a pseudo-2D profile, are presented in Fig. 3b. The deeper layer with resistivity of about 5 Ω·m below the lateral varying conductive layer has been interpreted as the clay-sand substratum of the aquifer, also in accordance with well perforations near the studied zone. Two 400 m-long Schlumberger VES soundings were carried out to confirm the presence of the deeper layer, with results compatible with the interpretation of TDEM soundings. An ARES instrument (GF Instruments, Czech Republic) was used for measurements, RES1DINV software for data interpretation.

Integrated data interpretation suggests that the saturated zone of the aquifer is affected by almost complete salt contamination up to 400-500 m from the coast line.

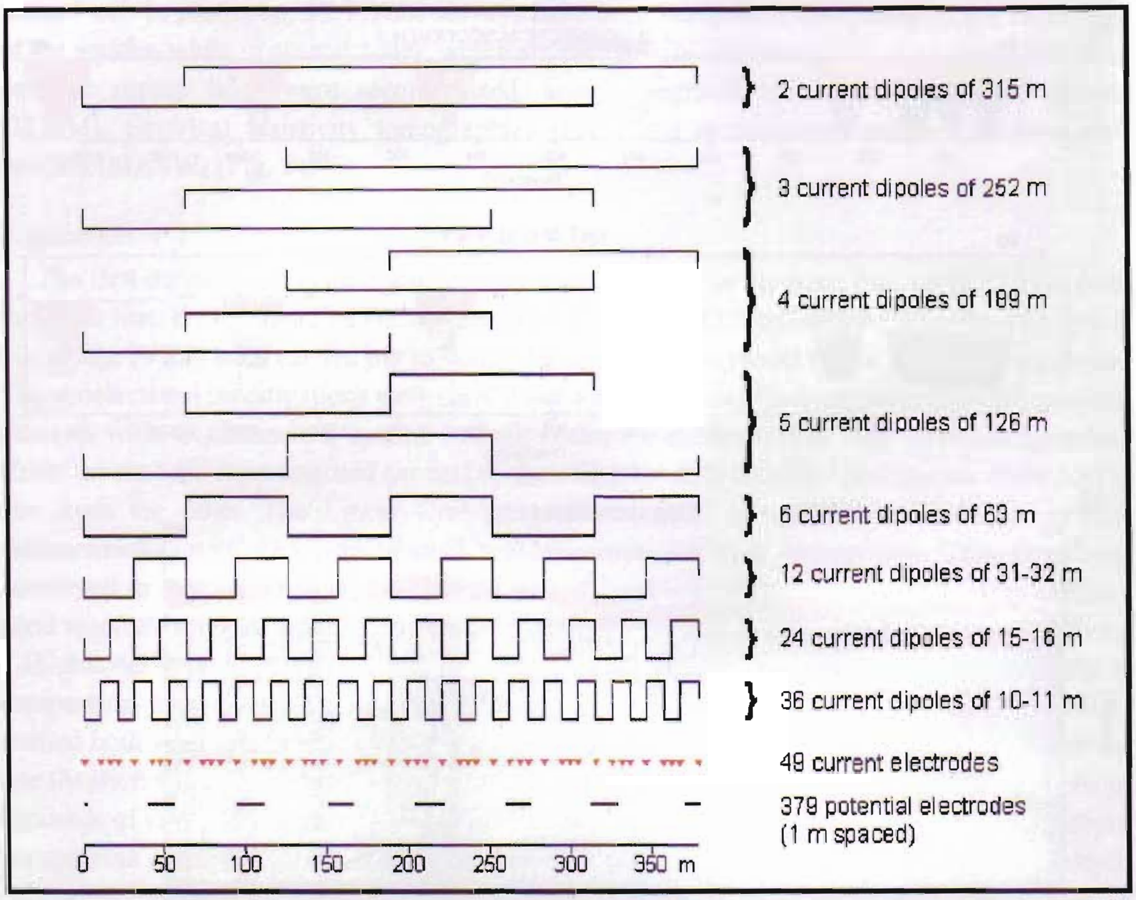

Fig. 4 - Acquisition sequence for ERT surveys in Section n°1.

2.2. *Section n° 2*

The second detailed survey line, 1400 m long, was carried out about 2 km from the first 2D survey line in a north-western direction. 13 TDEM soundings were performed along the line, while an electrical resistivity tomography with 379 electrodes, at 1 m spacings, was carried out. Finally 7 MASW profiles were acquired. The ERT sounding was carried out positioning the center of the investigation at about 500 m from the coast line, to try to intercept the lateral variation of resistivity due to the wedge of the sea intrusion (using the results of the first 2D survey as reference). The array used for measurements was again the Linear Grid, but with a different georesistivimeter. In fact, the MRS256 instruments (GF Instruments, Czech Republic) were used. The MRS256 instrument performs up to 256 potential simultaneous measurements, even if in the application presented here, it was used with only 64 channels. In fact, the instrument has been developed for 3D investigations: extensions for potential cables would be necessary to take full advantage of the multichannel capability of the instrument in 2D applications. The total amount of 379 electrodes of the profile were reached moving the 64 electrode cables six times along the profile. For each position of the potential cables, measurements with all the current dipoles of the acquiring sequence were performed, with current electrodes both inside and outside

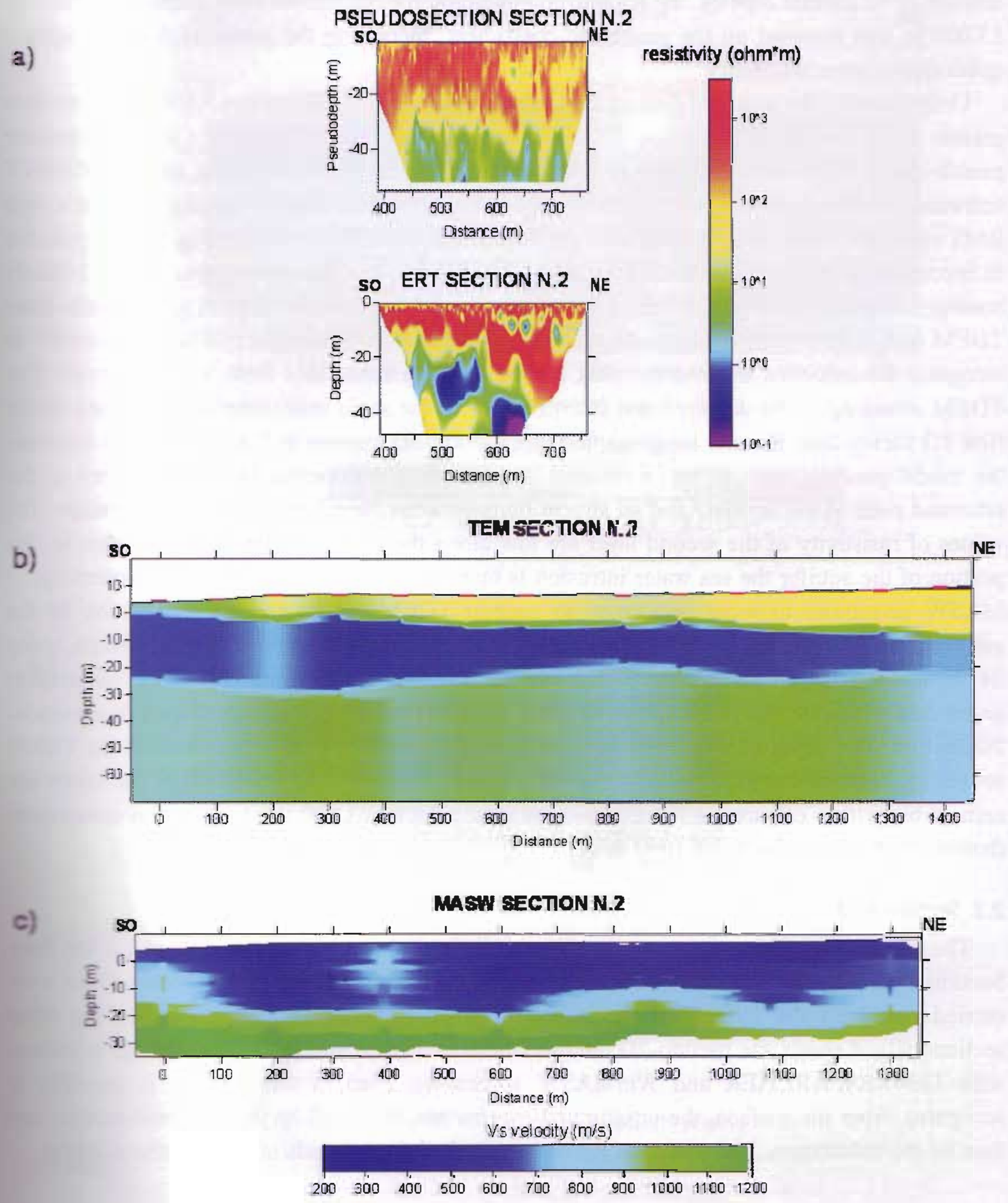

Fig. 5 - 2D interpretation of ERT survey (a), TEM soundings (b) and MASW measurements (c) relative to Section n°2.

the line covered by the 64 electrode cables. In this way, it was possible to obtain a tomography with 379 electrodes, and not the roll-along union of six different profiles. Fig. 4 shows the scheme of the acquisition sequence: 49 electrodes were used for current injection, for a total amount of 92 current dipoles. In this way about 15,500 measurements were acquired. A limit of 15,000 m was imposed on the geometric coefficient, increasing the potential dipole length of quadrupoles when necessary.

Unfortunately, the acquired data present a great noise content: only about 7,500 measurements present a standard deviation below 10%. Furthermore, the rejected data are those with greater pseudo-depth. For this reason, the inverted model (Fig. 5a), obtained again with RES2DINV software, reaches an investigated depth of about 45 m (1/8 of the profile length), presents a high RMS value and does not agree well with the TDEM and MASW soundings (Fig. 5). It is possible to recognize a resistive overburden on a saturated zone, but this latter layer is not laterally homogeneous and the depths of the contacts between layers do not correspond to the results from TDEM and MASW investigations. In the last hundreds of meters of the profile it is possible to recognize a conductive shallow anomaly, maybe due to a superficial fresh water reservoir. The TDEM soundings were acquired and interpreted with the same instrument and software of the first 2D survey line. Results are presented in a pseudo-2D manner in Fig. 5b. Even in this case the model presents three layers: a resistive overburden, a conductive layer (interpreted as the saturated zone of the aquifer) and an almost homogeneous deep layer, the clay substratum. The values of resistivity of the second layer are low along the entire profile, indicating that in this portion of the aquifer the sea water intrusion is more pronounced. Instead of VES soundings, 7 MASW investigations were performed to support TDEM results for the recognition of the substratum of the aquifer. MASW soundings were carried out with an ABEM seismograph, using 24 vertical 4.5 Hz geophones for each sounding. WinMASW software (Eliosoft) was used to invert data with a 2-layer model. The inversion models are shown in Fig. 5c, joined in a pseudo-2D section. The depth of the contact between the layers agrees well with that from the TDEM soundings between the saturated zone and the substratum. Even the velocities of the layers are compatible with a calcarenite layer (top layer with velocity of 500 m/s) and a clay substratum (bottom layer with velocity of 1000 m/s).

2.3. Section n° 3

The last section, 900 m long, was surveyed sub-parallel to the other two, about 1.3 km from Section n° 2 in a north-western direction: 6 TDEM soundings and 3 MASW investigations were carried out, with the same instruments and acquisition parameters described for the other sections. Fig. 6 shows the pseudo-2D interpretations of TDEM and MASW soundings (obtained with TEMRESEARCHER and WinMASW softwares): even in this case, it is possible to recognize, from the surface, the unsaturated overburden, followed by the saturated aquifer and then by the substratum. The wedge of the sea water intrusion extends inland for about 200 m.

3. 3D Reconstruction of the aquifer

The interpretations of the 53 TDEM soundings distributed in the area of the hydrogeological basin (instrument, acquisition parameter, and data analysis are the same described in the previous paragraphs), in conjunction with the results of the 42 investigations of the detailed profiles, were joined to construct a pseudo-3D model of the aquifer. Fig. 7 shows the 3D model divided into horizontal slices, for different altitudes above sea level. This graphical representation allows us to

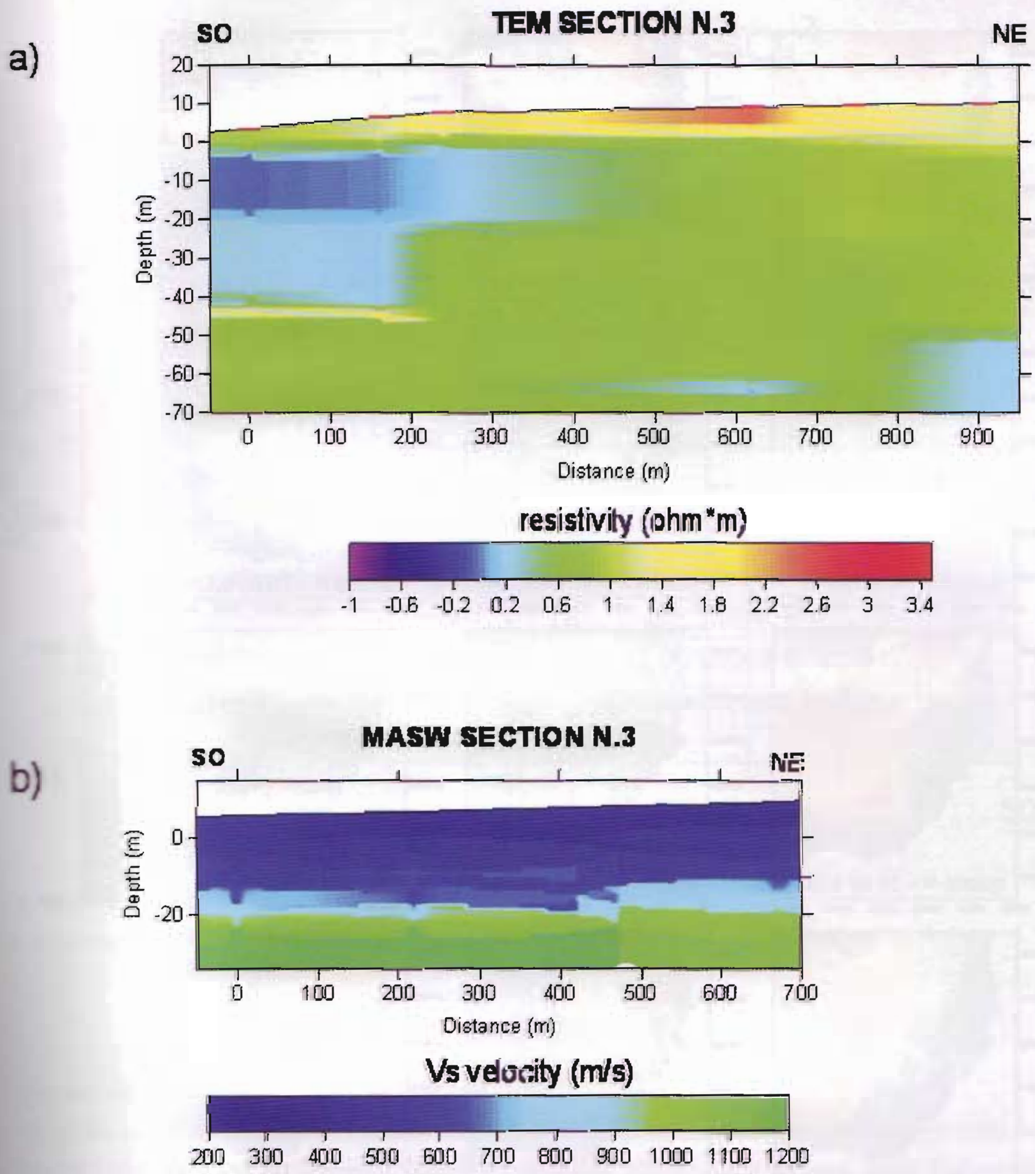

Fig. 6 - 2D interpretation of TEM soundings (a) and MASW measurements (b) relative to Section n°3.

define more accurately the main directions of sea water intrusion, comparing the results with information on the piezometric measurements taken from wells in the area.

The analysis of the results reveals the presence of extremely low (saturated zone) resistivity values increasing from the coast line inland and the sand-clay substratum in the entire studied area (beginning from 20 m of depth), with some preferential paths of sea water intrusion distinguishable near the coast line.

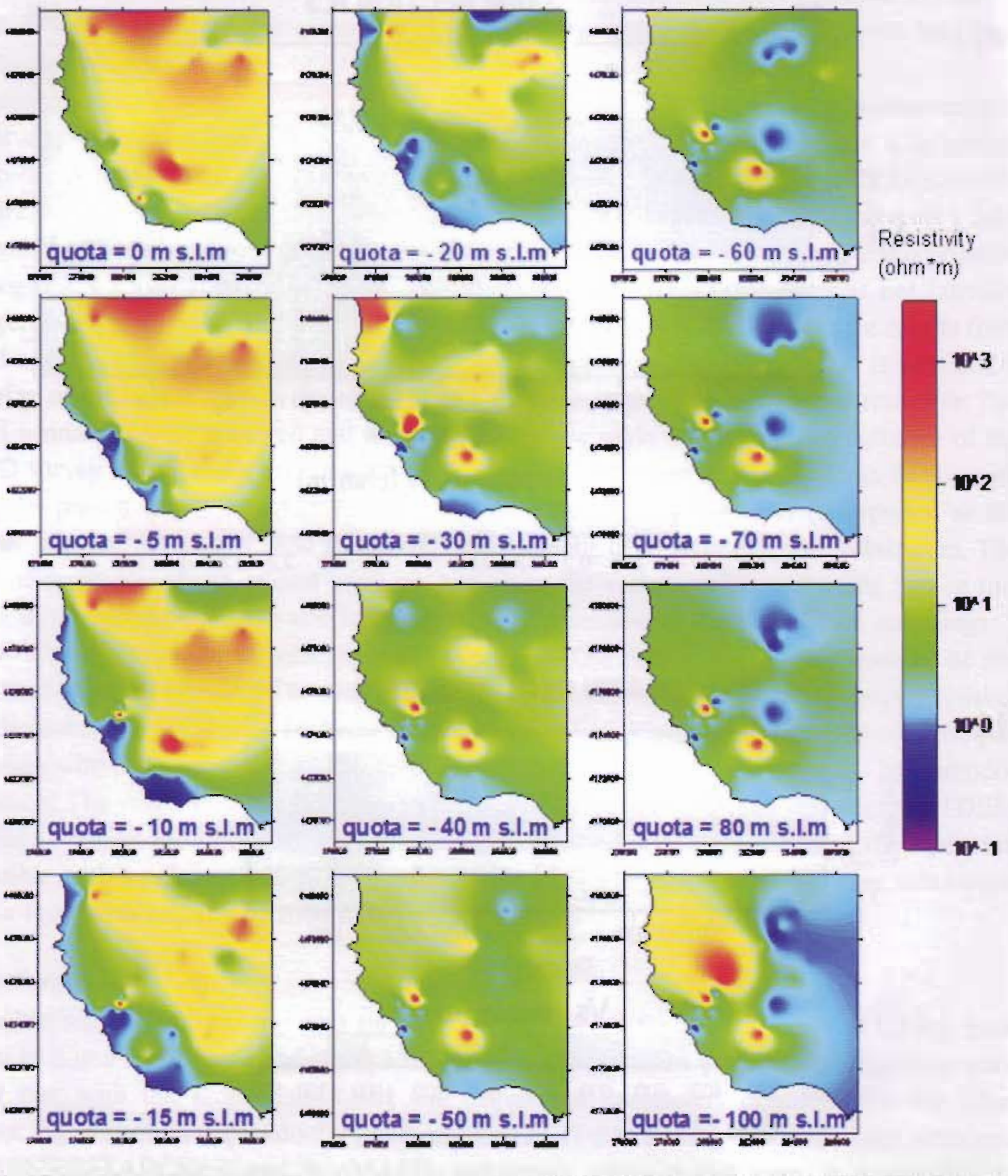

Fig. 7 - 3D model divided into horizontal slices, for different altitudes above sea level, obtained by 53 TEM surveys acquired in the area.

4. Geochemical survey

The characterization of the aquifer and the quantification of sea water intrusion by means of geophysical investigations, in particular in terms of geometric distribution of resistivity, imply two assumptions:

1. that the lateral variations of the resistivity values are related to the variations of the ion content of the water of the saturated zone (and then not strongly connected to variations of rock

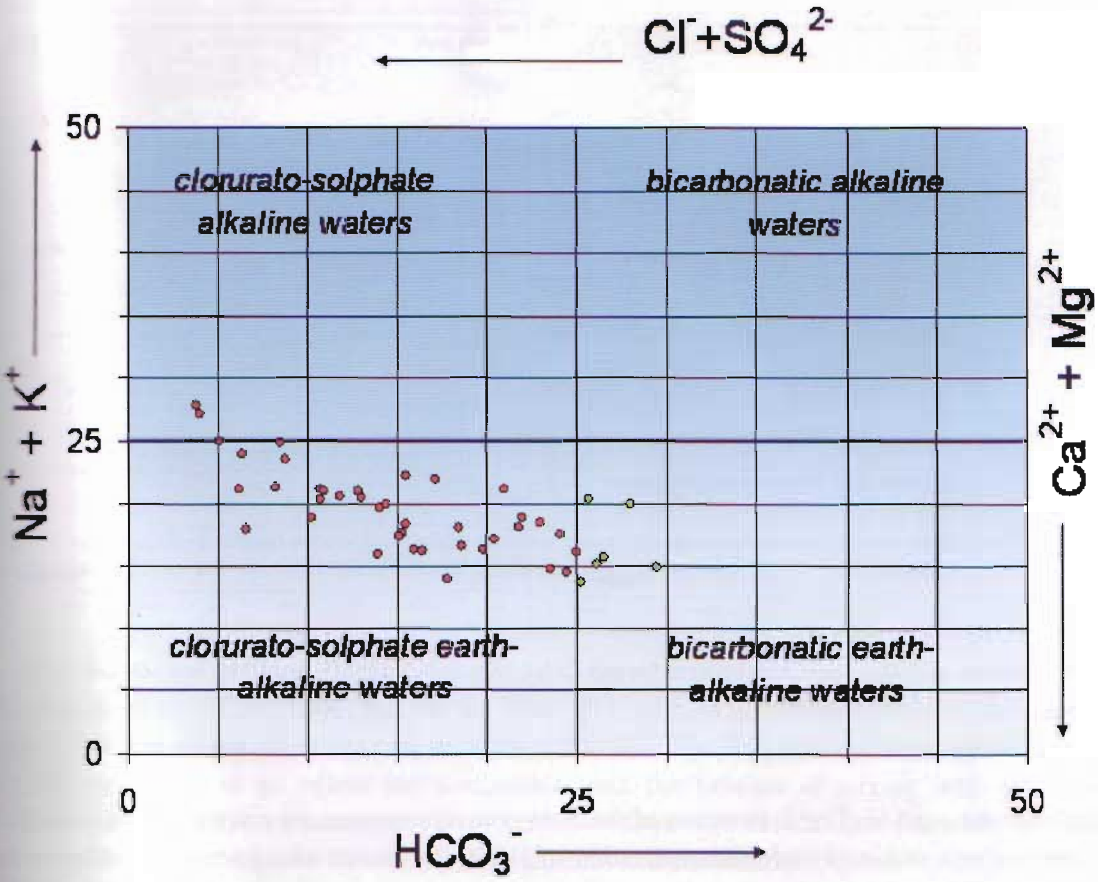

Fig. 8 - Langelier-Ludwig diagram for the classification of the sampled waters.

permeability and/or changes in lithological formations);

2. that the changes in the ion content of the groundwater depend on a mixing process with sea water (and then not on the significant presence of other contaminants, from the conductivity point of view).

The first assumption is linked to the geology of the aquifer, and is corroborated also by the stratigraphies and loggings of the wells of the investigated zone (Cosentino *et al.*, 2007). The second assumption can be proved by a geochemical survey, that gives also information on the contamination of the aquifer by chemicals other than salt water.

The water of 45 wells, selected in the most uniform way possible taking into account the wells' presence and accessibility (Fig. 2), was sampled and analyzed in a few days, in order to assure the consistency of results against temporal and climatic changes of water compositions. For each well, measurements of conductivity, pH, Eh, and temperature were carried out in situ, by means of portable instruments previously calibrated with standard solutions; the temperature was measured with an alcohol thermometer. The water was sampled by using the well pumps, if present; otherwise a sampling bottle was used. Different samples were taken for each water

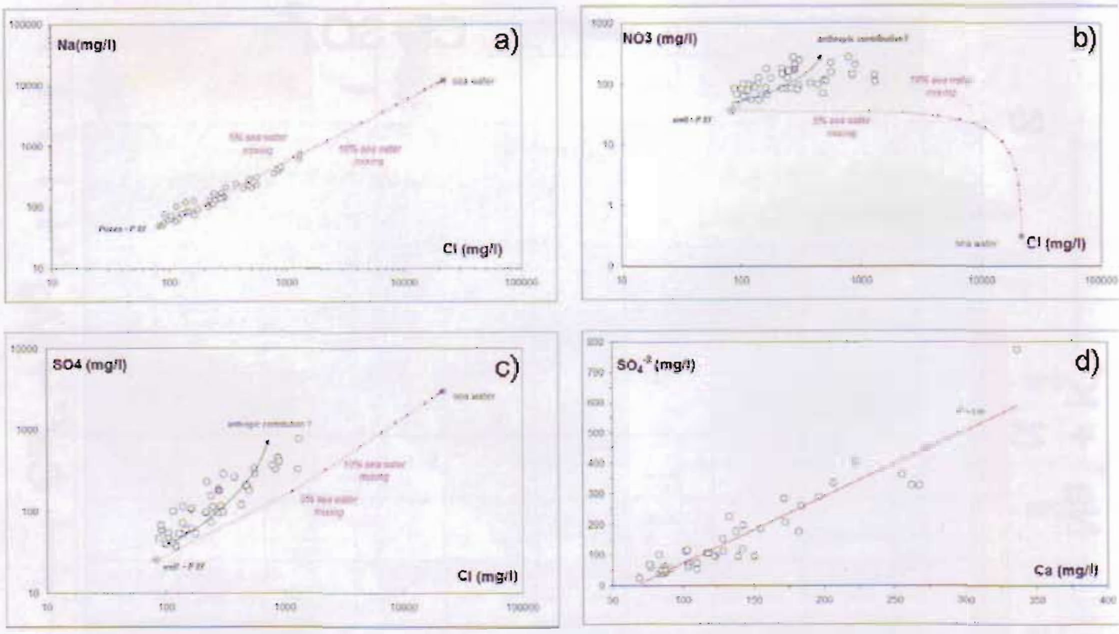

Fig. 9 - Graphics of binary correlation between Na and Cl (a), NO_3 and Cl (b), SO_4 and Cl (c) and SO_4 and Ca (d).

sample for the analytical determination of the main constituents: one for anions analysis, one for cations analysis and another for determination of HCO_3^- (by means of acid-based titration with HCl 0.1 N and methyl-orange as indicator; the samples were maintained refrigerated from the moment they were collected to the analysis). The samples for anions and cations analysis were filtered by 0.45 micron cellulose disposable Millipore filter. The sample for the cations analysis was acidified with HNO_3 to pH≈2, to prevent precipitation of insoluble salts.

5. Constituents analysis

The determination of the main constituents of the water samples were performed by Ionic Chromatography (IC). The chromatographer (Dionex DX 120) was equiped with a conductivity detector and columns containing a gel-type S-DVB resin. The pump of the chromatographer was set at 1500-2000 psi and the velocity of the flux of the solution at 1.2 ml/min. Fig. 8 shows the Langelier-Ludwig diagram for the classification of waters.

The samples analyzed fall mainly in the quadrant of clorurato-solphate Earth-alkaline waters, and show a weak tendency toward the first quadrant, where the mean composition of sea water is reduced. Only a few samples show a bicarbonatic main composition, maybe because these waters are the result of the interaction between rainwater and rocks, without a strong influence of sea intrusion and human contamination phenomena. Fig. 9 presents the graphics of binary correlation between Na and Cl (Fig. 9a), NO_3 and Cl (Fig. 9b), SO_4 and Cl (Fig. 9c) and SO_4 and Ca (Fig. 9d).

Cl and Na concentrations present a good correlation, indicating a process of mixing between

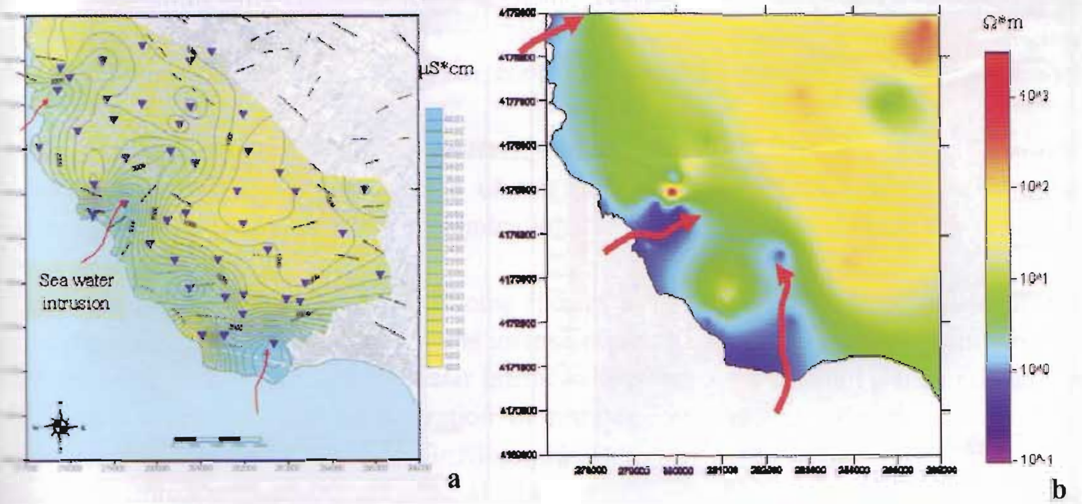

Fig. 10 - Map of the electrical conductivity of the sampled waters (a) in comparison with a depth slice of the pseudo-3D reconstruction of the resistivity distribution obtained by TDEM soundings (b).

the phreatic water (TDS<1000) and the sea water. This process influences almost all the samples, with a fraction of sea water content between 0 and 6%. The SO_4 concentration grows with Cl concentration, but at an extent not compatible with the process of mixing with sea water. Furthermore the SO_4 concentration is positively correlated with the Ca contents; often fertilizers for agriculture are composed by sulfates with calcium and ammonium (Agrawal *et al.*, 1999). The medium concentrations of nitrates and sulfates are respectively 117.2 mg/l and 160.5 mg/l, very much above Italian legislation limits (respectively 50 mg/l and 250 mg/l).

6. Spatial distribution of constituents

The map of the electrical conductivity of the sampled waters (Fig. 10), is presented as comparison to a depth slice of the pseudo-3D reconstruction of the resistivity distribution obtained by TDEM soundings. Well water reaches conductivity values of about 5000 μS/cm (at 25°C), about 1/10 of the typical conductivity of sea water (obviously the conductivity values are in accordance with the NaCl contents of the mixing curve of Fig. 9a). The resistivity values of the depth slice from TDEM soundings are not compatible with a contamination from sea water of up to 10%: the areas with resistivity of about 1 $\Omega\cdot$m or below represent an aquifer totally intruded by the sea. The contradiction between geophysical and geochemical analyses can be explained two ways. First of all the spatial sampling of the surveys are different, with well water sampling less close to the coastal line. Even if this arguement can explain some differences (for instance the discrepancy near the first 2D detailed geophysical section: the sea water infiltration is closer to the sea than the nearest sampled well), the inconsistency of the two approaches near the second detailed 2D geophysical section is not explainable this way: there is a sampled well really close to the line, and the sea intrusion evaluated from a geophysical standpoint extends for more than 1 km from the coastal line. The discrepancy can be justified considering that the

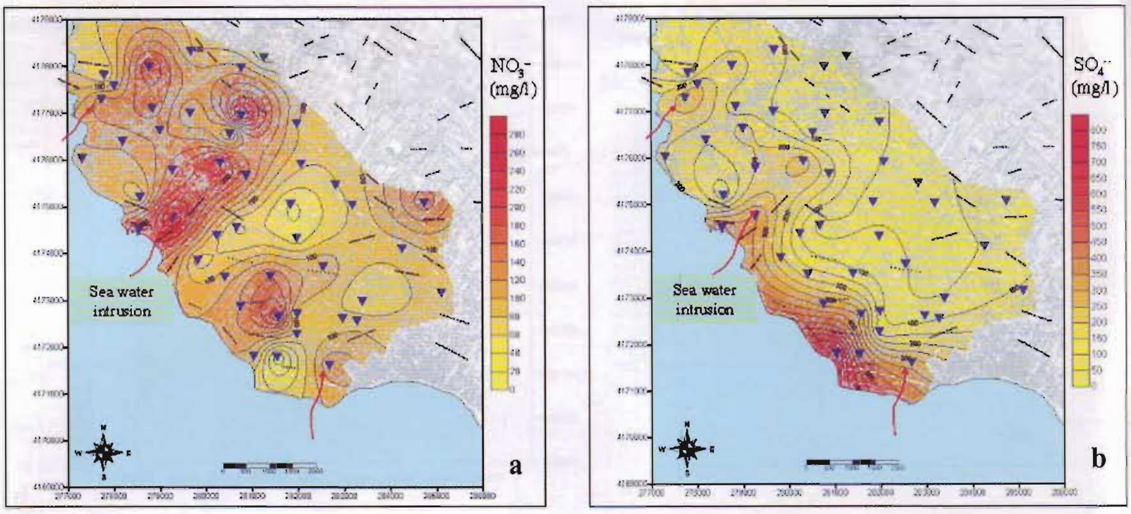

Fig. 11 - Maps of nitrate contaminants (a) and maps of sulfate contaminants (b).

aquifer under study is a multilayer aquifer, and that the water table of the sampled well near the 2D section is 10 m above sea level, while the resistivity depth slice is 15 m below sea level: the sampled water, and its mixing content with sea water, probably refer to shallower groundwater. This consideration is in accordance with the presence, in the ERT profile of section 2, of a conductive anomaly in the resistive overburden above the sea level (see Fig. 5a).

Fig. 11 shows the spatial distribution of nitrate and sulfate concentration. The nitrate contaminants usually originate from human activity: in fact, there is a good correlation between the higher values of contaminants and the areas with higher population and/or cultivation density. Although these distribution maps show little correlation with the geophysical data, however, the sulfates distribution is apparently affected by the sea water intrusion phenomenon. Probably because the sulfates distribution and the sea water intrusion are both related to the low permeability areas of the aquifer.

7. Conclusion

The results of the geophysical and hydrogeochemical surveys allowed us to check, implement and partially support the previous hydrological balances of the coastal aquifer of Marsala-Mazara del Vallo (Cosentino *et al.*, 2007).

The integration of the selected geophysical and geochemical methodologies allowed us to decrease the uncertainty limits of the various inversions, by means of a superposition of the various geometrical models obtained.

Some uncertainties do still remain: they are related to the real exploitation of the area and to the comparison of such utilisation with both the officially and unofficially declared utilization.

The implementation of an integrated geophysical survey (ERT, TEMFAST and seismic type MASW) along three of the preferential directions of marine intrusion, allowed us to obtain sections of great detail in an area of interest, defining, with precision, the geometry of the wedge of sea water intrusion and the transition zone. The data obtained from different methodologies, confirm all sections of detail investigated, the reconstruction of the physical-mathematical model obtained for the whole investigated area.

The geochemical composition of the water shows the chemical-physical and compositional parameters attributable to the intervention of two different processes: a sea water intrusion phenomena and a process of anthropic contamination due to percolation of fertilizers or of waste-water rich in nitrates.

In particular, the high content in these ionic species in this area, partly coinciding with the town of Petrosino, are caused not only by the intense exploitation of groundwater, from which a more pronounced phenomenon of sea water intrusion follows, but also from a high population density, which implies a high concentration of nitrates from leaking of fertilizers used in cultivations, very common in this area (Griffioen, 2001).

This work, from a methodological point of view, could represent a standard for investigations in coastal areas that suffer problems of sea water intrusion.

REFERENCE

Agrawal G.D., Lunkad S.K. and Malkhed T.; 1999: *Diffuse agricultural nitrate pollution of groundwaters in India.* Water Sci. Technol., **39**, 67–75.

Archie G.E.; 1942: *The electrical resistivity log as an aid to determining some reservoir characteristics.* Trans AIME, **146**, pp. 54-63.

Cosentino P., Capizzi P., Fiandaca G., Martorana R., Messina P. and Pellerito S.; 2007: *Study and monitoring of salt water intrusion in the coastal area between Mazara del Vallo and Marsala (South-Western Sicily).* In: Rossi G., Vega T. and Bonaccorso B. (eds). Methods and Tools for Drought Analysis and Management, Series: Water Science and Technology Library, Vol. **62**., XVI, Springer, ISBN: 978-1-4020-5923-0, pp. 303-321.

D'Angelo U. and Vernuccio S.; 1992: *Carta geologica del Foglio 617 "Marsala" scala 1:50000.* Boll. Soc. Geol. It., **113**.

Edwards L.S.; 1977: *A modified pseudo-section for resistivity and induced-polarization.* Geophysics, **42**, 1020-1036.

Fiandaca G., Martorana R. and Cosentino P.L.; 2005: *Use of the linear grid array in 2D resistivity tomography.* In: Proceedings of the Near Surface 2005 - 11th European Meeting of Environmental and Engineering Geophysics, Palermo, 4-7 September 2005, A023, ISBN: 90-737-819-4, 4 pp.

Fitterman D.V. and Stewart M.T.; 1986: *Transient electromagnetic sounding for groundwater.* Geophysics, **51**, 995–1005, doi:10.1190/1.1442158.

Goldman M., Gilad D., Ronen A. and Melloul A.; 1991: *Mapping of seawater intrusion into the coastal aquifer of Israel by the time domain electromagnetic method.* Geoexploration, **28**, 153–174, doi:10.1016/0016-7142(91)90046-F.

Griffioen J.; 2001: *Potassium adsorption ratios as an indicator for the fate of agricultural potassium in groundwater.* J. Hydrol., **254**, 244–254.

Hoekstra P. and Blohm M.V.; 1990: *Case histories of time-domain electromagnetic soundings in environmental geophysics.* In: Ward S.H. (ed), Geotechnical and Environmental Geophysics (SEG Book Mart, Academic Series vol. 2), pp. 1–15.

Janz G.J. and Singer S.K.; 1975: *Copenhagen standard sea water: conductivity and salinity.* Journal of solution chemistry, **4**, 995-1003, doi: 10.1007/BF01074741, ISSN: 0095-9782 (print).

Kafri U., Goldman M. and Lang, B.; 1997: *Detection of subsurface brines, freshwater bodies and interface configuration in-between by the time domain electromagnetic method in the Dead Sea Rift, Israel.* Environmental Geology, **31**, 42-49, doi: 10.1007/s002540050162.

Martorana R., Fiandaca G., Casas Ponsati A. and Cosentino P.L.; 2009: *Comparative tests on different multi-electrode* *arrays using models in near-surface geophysics*. Journal of Geophysics and Engineering, **6**, 1-20, doi: 10.1088/1742-2132/6/1/001.

National Research Council; 2000: *Clean coastal waters - Understanding and reducing the effects of nutrient pollution*. Washington, D.C., National Academy Press, 405 pp.

Park C.B., Miller R.D. and Xia J.; 1999: *Multi-channel analysis of surface waves*. Geophysics, **64**, 691-700, doi:10.1190/1.1444590.

Xia J., Miller R.D. and Park C.B.; 1999: *Estimation of near-surface shear-wave velocity by inversion of Rayleigh wave*. Geophysics, **64**, 691-700, doi:10.1190/1.1444578.

Yang C.H., Tong L.H. and Huang C.F.; 1999: *Combined application of dc and TEM to sea-water intrusion mapping*. Geophysics, **64**, 417-425, doi:10.1190/1.1444546.

Corresponding author: Patrizia Capizzi
Department of Chemistry and Physics of the Earth (CFTA), University of Palermo, Italy
via Archirafi 26, 90133 Palermo, Italy
phone: +39 091 23861611; fax: +39 091 6177580; e-mail: patrizia.capizzi@unipa.it